Available online at www.sciencedirect.com
SCIENCE DIRECT®
Journal of Magnetic Resonance 174 (2005) 338–342
JMR Journal of Magnetic Resonance
www.elsevier.com/locate/jmr

Communication

Stray field measurements of flow displacement distributions without pulsed field gradients

U.M. Scheven *

Schlumberger Cambridge Research, High Cross, Madingley Road, Cambridge CB3 0EL, UK

Received 19 November 2004; revised 25 January 2005
Available online 1 April 2005

Abstract

The probability distribution $P(\zeta)$ of diffusive and advective molecular displacements is determined using a fixed field gradient (FFG) pulse sequence, on fluid flow through a Bentheimer sandstone, in the grossly inhomogeneous stray field of a super-conducting magnet. Two decades of q-space are scanned with stimulated echoes, using the gradient of the stray field and variable encoding times δ. The strength of the gradient permits the use of short encoding times, which is desirable for limiting the distorting effects produced by flow displacements through susceptibility induced field inhomogeneities. CPMG and CP echo trains are used to refocus separately the real and imaginary parts of the stimulated echo, for experimental efficiency.

PACS: 47.55.Mh

Keywords: Stray field; Propagator; Flow; Rocks

1. Introduction

Flow in porous media is commonly studied using pulsed field gradient (PFG) NMR techniques [1–3], where pulsed external field gradients are applied to encode the displacement of spins during some evolution time Δ in the phase θ of their magnetization. The displacement distribution, also referred to as the volume averaged propagator, can be extracted from such data by Fourier transform. This paper presents an analogous fixed field gradient (FFG) method suitable for flow measurements in samples located outside of an NMR apparatus, say in the stray field of an unshielded super-conducting magnet, a well logging tool, or an NMR mouse [4], where a static field gradient of several mT/m can be present. The viability of the method discussed here is demonstrated with measurements of the volume averaged displacement probability distribution of molecular displacements in Stokes flow through a rock core.

NMR in stray fields has found many applications where the sample is located outside the NMR apparatus, for example in well logging [5], materials testing and quality control [6], stray field imaging [4], and stray field measurement of velocity distributions [7]. The CPMG-experiment ($(\pi/2)_x$–$[\tau$–π_y–τ–$]^n$) is the prototypical sequence for stray field work because it offers advantages in the signal-to-noise ratio (SNR), and because it can be used to probe relaxation and diffusion properties of the sample. Its spin dynamics in grossly inhomogeneous fields are well understood [8,9], and it is used in logging applications for the measurement of T_2-relaxation time distributions. CPMG-like sequences [10] have been introduced in two-dimensional stray field experiments probing diffusion–relaxation (D–T_2) correlations and relaxation–relaxation (T_1–T_2) correlations, where 'editing' sequences sensitive to diffusion or T_1-relaxation

* Fax: +44 1223467004.
E-mail address: scheven@slb.com.

1090-7807/$ - see front matter © 2005 Elsevier Inc. All rights reserved.
doi:10.1016/j.jmr.2005.03.003

replace the standard π/2 excitation pulse of the CPMG-sequence. More recently PFG-CPMG/CP stray field imaging experiments [4] have been developed, where the 'editing' sequence consists of the standard PFG spatial encoding, followed by CPMG and CP echo trains measuring real and imaginary parts of the NMR signal. In this work, we employ a pulse sequence belonging to the 'editing' family of stray field sequences, sharing salient features with the (D–T_2)-editing sequence and the stray field imaging sequences referred to above. Below we discuss our experimental setup, the pulse sequence, and the data acquired with it. Our experiments demonstrate how to measure volume averaged molecular displacement distributions efficiently and without pulsed field gradients, in the extremely inhomogeneous fields of a stray field NMR geometry. We present results obtained on water in Bentheimer rock core, with and without flow, and discuss some limitations of the technique, comparing data obtained in a stray field with the equivalent data obtained using standard PFG methods in a homogeneous field at 83 MHz.

2. Experimental

A cylindrical Bentheimer sandstone core was sealed on its circumference with epoxy, and fluid distributor caps were attached to the ends of the core and then connected to a flow system. Axial flow of water through the core was driven by a ISCO-1000D piston pump. Experiments were conducted in the absence of flow and for a flow rate of $\langle v\rangle = 0.5$ mm/s. The core was placed within a 1.765 MHz solenoid NMR probe, located in the fringe field of a super-conducting magnet, where the field $\|\mathbf{B}_0\| = 41.4$ mT and the gradient $\|\mathbf{g}\| = 13.8$ mT/m at the center of solenoid. The axes of solenoid, rock core, and gradient were co-linear, and hence the direction of flow and of the field gradient were co-linear as well.

The pulse sequence is shown in Fig. 1. It is based on the STE-CPMG diffusion editing sequence introduced in [10]. Three π/2 pulses produce a stimulated echo $S(q)$ at time $T_e = \Delta + 2\delta$. Signals associated with unwanted coherence pathways are eliminated by phase cycling

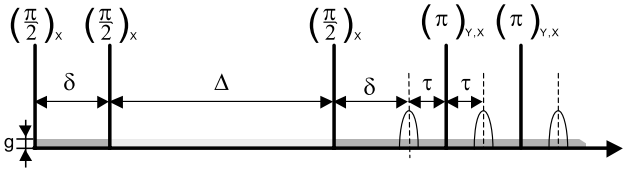

Fig. 1. A stimulated echo at $T_e = \Delta + 2\delta$ encodes displacement. With CPMG phase cycling the $(\pi)_y$ pulses re-focus the real part of the stimulated echo. With CP phase cycling $(\pi)_x$ pulses refocus the imaginary part of the stimulated echo. The fixed background gradient is indicated in dark grey, for intervals where magnetization is in the xy-plane.

[10] or were reduced below detection level by diffusion in the external gradient, or both.The ensemble average $S(q) = \langle e^{iq\zeta_j}\rangle$ is taken over all magnetized spins j displaced by ζ_j in the interval $\Delta + O(\delta)$ between the first and third π/2-pulse, and therefore it is recognized as the qth Fourier component of the displacement distribution, if the effects of relaxation and internal fields can be ignored [11]. $S(q)$ is measured, as in the classic PFG experiments [1–3], over a suitable range $\{q\}$ of q-space, where $q = \gamma\delta g$, γ is the proton gyromagnetic ratio, δ is the duration of the gradient encoding period, and g is the amplitude of the stray field gradient.

For experimental efficiency the signal is refocussed and measured with 2000 CPMG/CP spin echoes. It has been shown [8] that asymptotically in grossly inhomogeneous fields only a y-component of the initial magnetization is re-focussed by the π_y-pulses of the CPMG sequence, while the orthogonal x-component of the magnetization, and hence all phase information, is lost. Therefore, the complex stimulated echo signal $S(q)$ is measured with echo trains using CPMG and CP phase cycles, where for the CP phase cycle the phase of the refocussing π-pulse was rotated by 90° with respect to that of the CPMG echo train. A complex echo train $S'(q,t)$ is then obtained by adding the real part of the CPMG echo train to imaginary part of the CP echo train, for each choice of $q = \gamma\delta g$. The echo trains are summed to determine the stimulated echo $S(q)$. Measurements are performed for 30 logarithmically spaced values of δ between 20 μs and 3 ms, with $\Delta = 280$ ms, and the ensemble averaged displacement distribution $P(\zeta)$ is then determined by Fourier transform of the measured set $\{S(q)\}$.

Standard PFG experiments employing the 13-interval alternating pulsed field gradient sequence [3] (APGSTE) were performed to compare with our stray field results, using the same sample, flow rate, and evolution time Δ.

3. Results

Fig. 2 shows the real and imaginary parts of the magnetization decay $S'(q,t)$ acquired with CPMG and CP echo trains, in the presence and absence of flow, for three representative choices of q. The time of the first recorded echo defines $t = 0$ for these plots. We first focus on the stagnant case shown in the panels on the left. The imaginary part of the echo trains shown in Fig. 2C is zero because we have used the average phase of measurements performed in the absence of flow to define the single reference phase used for all measurements. The phase is independent of q, as expected for diffusive displacements. In Fig. 2A the signal for the largest choice of q is reduced below the noise level because the stimulated echo $S(q) \propto \exp\{-q^2 D(\Delta + \frac{2}{3}\delta)\} \ll 0.01$. Such diffusive attenuation is absent for the two smaller

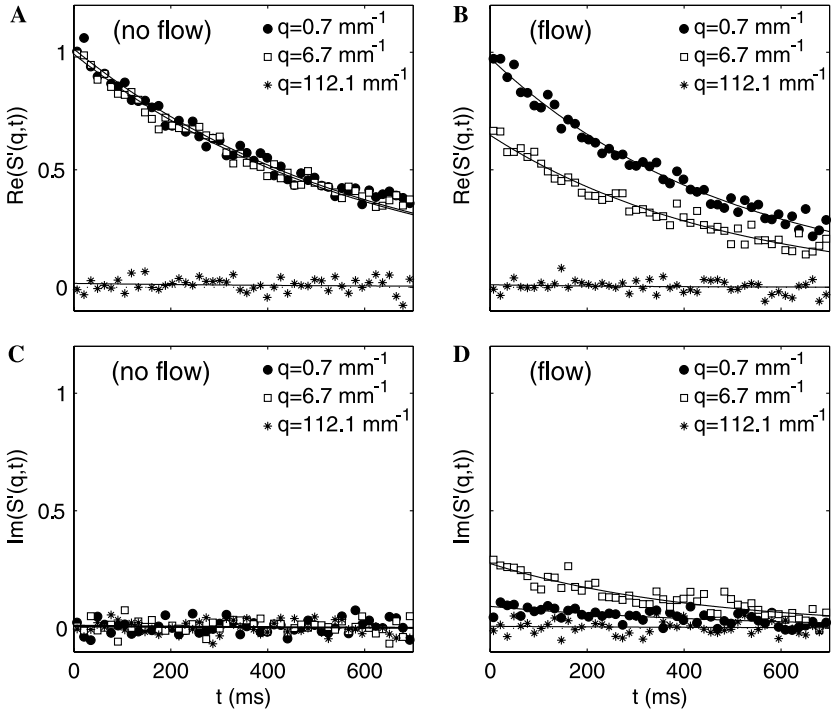

Fig. 2. T_2-decay of the real part the stimulated echo, without (A) or with flow (B), for three representative choices of q. T_2-decay of the imaginary part without (C) and with flow (D) for the same choices of q. Each data point contains 40 binned echoes, solid lines show exponential fit to the data.

choices of $q = 0.7\ \mathrm{mm}^{-1}$ and $q = 6.7\ \mathrm{mm}^{-1}$ for which the experiment probes displacements of order $2\pi/q \gg l_D = \sqrt{2D\Delta}$. Figs. 2B and 2D show the results of the same experiment, conducted in the presence of flow. Now the NMR signal does acquire an imaginary component, as shown in Fig. 2D, for $q = 0.7\ \mathrm{mm}^{-1}$ and more prominently so for $q = 6.7\ \mathrm{mm}^{-1}$, where the experiment probes displacement length scales approaching the mean displacement $\langle\zeta\rangle_0 = \langle v\rangle\Delta$. Additionally for $q = 6.7\ \mathrm{mm}^{-1}$ the real part of $S'(q,t)$ is reduced, as shown in Fig. 2B. The rotation of the phase and attenuation of the magnitude of the NMR signal are a typical [12,13] NMR-signatures of flow familiar from displacement encoding PFG experiments. The solid lines in Fig. 2 show exponential fits to the data which decays with $T_2 \approx 500$ ms for all q. The single exponential fits are reasonably good, and therefore a straight sum of echo amplitudes $S'(q,t)$ provides a simple measure of the stimulated echo $S(q)$.

Fig. 3A shows $S(q)$ vs. q in the absence of flow, plotted with solid symbols. Negative q are not accessible experimentally and hence we plot $S(-q) = S^*(q)$ with open symbols, along with the data point at $S(0)$, which is obtained by extrapolation near $q = 0$. In the absence of flow diffusion shapes the q dependence of $S(q)$, as shown in Fig. 3A. It is approximately gaussian, as is the corresponding displacement distribution $\mathbf{P}(\zeta)$ produced from it by Fourier transform, as shown in Fig. 3C. The equivalent distribution obtained by conventional (APGSTE) pulsed field gradient experiments at 83 MHz coincides with and confirms the stray field result. We note that the measured diffusive $\mathbf{P}(\zeta)$ are narrower and more sharply peaked than the strictly gaussian propagator calculated for free diffusion of water with $D = 2.1\ \mu\mathrm{m}^2/\mathrm{ms}$ and $\Delta = 280$ ms which is shown for comparison with a dotted line in the same panel. This reduction is attributed restricted diffusion in the pore space [14]. In the presence of flow the picture changes. Figs. 3B and 3D show the corresponding $S(q)$ and displacement distribution obtained for $\langle v\rangle = 0.5$ mm/s, under the same experimental conditions and using the same pulse sequences, reference phase and normalization values as were used in the stagnant case. Now $S(q)$ has the typical dispersive appearance known from PFG-propagator experiments, where on a scale set by $\|q\| = 2\pi/\langle\zeta\rangle_0$ the imaginary part of the signal grows and then shrinks again with increasing q, as flow rotates and then scrambles the signal. For larger $\|q\|$ the signal appears as diffusive wings flanking the central region. The displacement distribution obtained from these data is shown in Fig. 3D, along with the equivalent result obtained by conventional (APGSTE) experiments at 83 MHz. They are rather similar but not identical. Both show a stagnation peak centered around zero displacement, with a shoulder corresponding to the displaced molecules for positive ζ. The stagnation peak of the displacement distribution obtained in the stray field is larger than in the one obtained by PFG techniques, while the amplitude of the displacement shoulder is

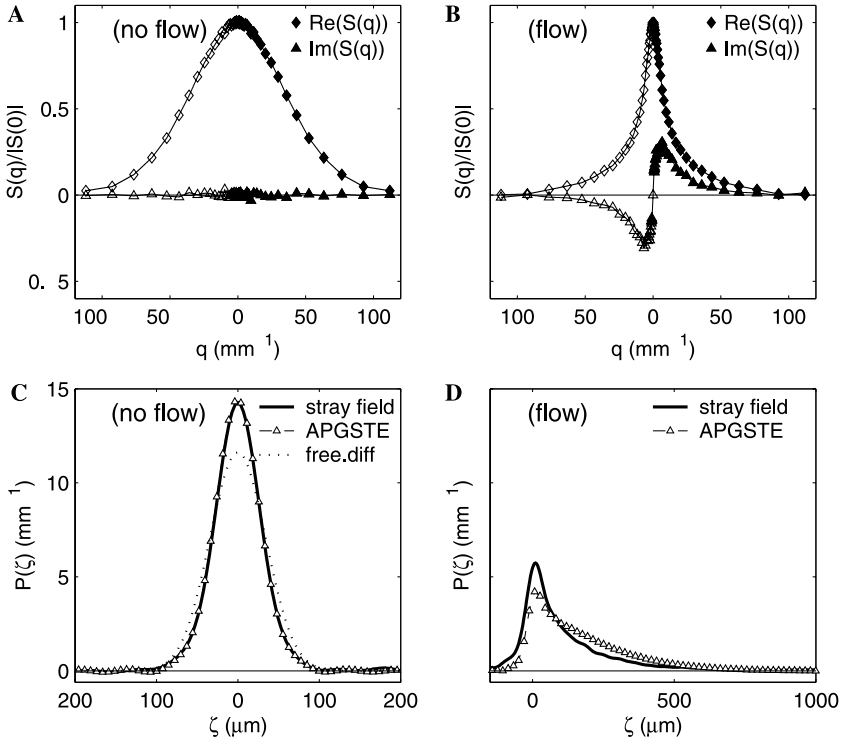

Fig. 3. $S(q)$ vs. q, without (A) or with flow (B). Data shown with solid symbols, hollow symbols show $S(-q) = S^*(q)$ and $S(0)$ obtained by extrapolation of data near $q = 0$. $\mathbf{P}(\zeta)$ vs. ζ, obtained by Fourier transform of data at top, without (C) or with (D) flow. The equivalent APGSTE results are indicated by open triangles.

smaller. The measured displacement in the stray field is therefore somewhat less than that measured with PFG. Possible causes for this discrepancy will be discussed below.

4. Discussion

The results presented here demonstrate the measurement of diffusion and flow displacement distributions in a stray field with fixed gradient g. The experiment systematically varies the time δ during which the excited magnetization is sensitive to g, permitting a measurement of the the qth Fourier component $S(q)$ of the displacement distribution. The strong external gradient of the inside-out NMR geometry has allowed the use of short encoding times, which is useful for flow measurements in magnetically heterogeneous systems, such as the rock used here. However, the range of q over which the experiment can be conducted and analyzed in the manner presented here is bounded from above by the requirement that $\delta \ll \Delta$, and from below by finite pulse width considerations: in our analysis we have implicitly assumed rectangular RF-pulses of negligible width and neglected the probe's ring-down and finite rise times. For the smallest $\|q\|$ these approximations may be too crude when the encoding period δ becomes comparable to the pulse duration $t_{\frac{\pi}{2}} = 12\ \mu s$ or the ring down time $t_r \approx 10\ \mu s$ of the NMR probe, or both. In this case $q = \gamma\delta g$ may no longer hold, and the approximation that it does may be the cause for the observed distortion of the stray field flow displacement distribution $P(\zeta)$, because it is precisely the small-$\|q\|$ measurement which probes length scales on the order of the width and mean displacement of $P(\zeta)$. By contrast the diffusive propagator is not affected by small $\|q\|$ effects, because here $S(q) \approx 1$ is almost independent of q for small q, as is evident from Figs. 2A and 3A. It is worth pointing out that the small-$\|q\|$ issues discussed here can be circumvented by either probing smaller mean displacements, attainable by reducing either Δ or $\langle v \rangle$, by working with smaller fixed gradients g, or arranging the experimental geometry such that there is a finite angle between the direction of mean flow and the gradient, whence only a component of displacements parallel to the gradient will be measured.

Other effects, such as surface relaxation, internal field offsets, and flow induced displacements through these internal fields can distort propagator measurements [11], whether they are measured in stray fields or homogeneous fields using PFG techniques. These distorting effects may depend on the applied field $\|\mathbf{B_0}\|$, and this, too, may account for some or all of the observed discrepancy between our flow results obtained in the stray field at 1.765 MHz and those measured by APGSTE at 83 MHz.

5. Conclusion

We have performed measurements of volume averaged diffusive and flow propagators in the fringe field of a super-conducting magnet, without using pulsed field gradients. The measurement is sensitive to molecular displacements along the direction of the fixed field gradient. The strength of the fixed gradient leads to spin dynamics requiring separate experiments to efficiently measure the real and imaginary parts of the stimulated echo, using CPMG and CP echo trains. The strong fixed gradient also makes it possible to cover a suitable range of q space using short encoding intervals, on the order of few milliseconds, which is comparable with encoding times commonly used in standard NMR imaging. Reasonably good quantitative agreement between stray field results and equivalent results obtained using conventional pulsed field gradient methods suggest that the technique could be developed further and used for quantitative measurements of volume averaged propagators in single-sided NMR geometries, for example in well-logging applications or in industrial flow monitoring and process control applications.

Acknowledgment

We thank Martin Hürlimann for useful discussions.

References

[1] E.O. Stejskal, J.E. Tanner, Spin diffusion measurements: spin echoes in the presence of a time dependent field gradient, J. Chem. Phys. 42 (1) (1965) 288–292.

[2] J. Kärger, W. Heink, The propagator representation of molecular transport in microporous crystallites, J. Magn. Reson. 51 (1) (1983) 1–7.

[3] R.M. Cotts, M.J.R. Hoch, T. Sun, J.T. Markert, Pulsed field gradient stimulated echo methods for improved NMR diffusion measurements in heterogeneous systems, J. Magn. Reson. 83 (2) (1989) 252–266.

[4] J. Perlo, F. Casanova, B. Blümich, 3D imaging with a single-sided sensor: and open tomograph, J. Magn. Reson. 166 (2004) 228–235.

[5] R.L. Kleinberg, A. Sezginer, D.D. Griffin, M. Fukuhara, Novel apparatus for investigating an external sample, J. Magn. Reson. 97 (1992) 466–485.

[6] G. Eidman, R. Salvelsberg, P. Blümler, B. Blümich, The NMR-MOUSE, a mobile universal surface explorer, J. Magn. Reson. A 122 (1996) 104–109.

[7] F. Casanova, J. Perlo, B. Blümich, Velocity distributions measured remotely with a single-sided NMR sensor, J. Magn. Reson. 171 (2004) 124–130.

[8] M.D. Hürlimann, D.D. Griffin, Spin dynamics of Carr–Purcell–Meiboom–Gill-like sequences in grossly inhomogeneous B_0 and B_1 fields and application to NMR well logging, J. Magn. Reson. 143 (1999) 120–135.

[9] M.D. Hürlimann, Diffusion and relaxation effects in general stray field experiments, J. Magn. Reson. 148 (2001) 367–378.

[10] M.D. Hürlimann, L. Venkataramanan, Quantitative measurement of two-dimensional distribution functions of diffusion and relaxation in grossly inhomogeneous fields, J. Magn. Reson. 157 (2002) 31–42.

[11] U.M. Scheven, J.G. Seland, D.G. Cory, NMR-propagator measurements on flow through a random pack of porous glass beads and how they are affected by dispersion, relaxation and internal field inhomogeneities, Phys. Rev. E 69 (2004) 021201-1-9.

[12] A. Sodickson, D.G. Cory, A generalized k-space formalism for treating the spatial aspects of a variety of of NMR experiments, Prog. NMR Spectrosc. 33 (2002) 77–108.

[13] P.T. Callaghan, Principles of Nuclear Magnetic Resonance Microscopy, Clarendon, Oxford, 1991.

[14] P.P. Mitra, P.N. Sen, L.M. Schwartz, P. LeDoussal, Diffusion propagator as a probe of the structure of porous media, Phys. Rev. Lett. 68 (1992) 3555.